Int J Earth Sci (Geol Rundsch) 95:1039–1052
DOI 10.1007/s00531-006-0088-4

ORIGINAL PAPER

Structure, age and mode of emplacement of the Hercynian Bordères-Louron pluton (Central Pyrenees, France)

Gérard Gleizes · Gérard Crevon · Asfawossen Asrat · Pierre Barbey

Received: 20 March 2005 / Accepted: 6 March 2006 / Published online: 31 May 2006

Abstract The Hercynian Bordères-Louron pluton (20 km^2) in the Central Pyrenees intrudes Devonian and Carboniferous metasediments. It shows a concentric zoning and consists of a significant proportion of (quartz) gabbros in its periphery, and of granodiorites, biotite monzogranites and biotite-muscovite monzogranites in its core. AMS study shows that the pluton corresponds to an elongated dome with a N100°E-trending axis. The anisotropy intensity Ppara% is high in the south and in the core of the pluton, whereas it is low in the north. The shape parameter *T* indicates that the fabric is strongly planar in a large central band oriented NW-SE, whereas it is strongly linear in the western and eastern tips of the pluton. These characteristics suggest that the Bordères-Louron pluton emplaced in two episodes: (1) intrusion of mafic magmas along a N100°E sill parallel to the regional foliation of the host metasediments; and (2) injection of three successive silicic batches (granodiorite, biotite monzogranite, two-micas monzogranite) which pushed aside the early mafic injections. In situ U-Pb dating of zircon grains indicates that the emplacement age of the biotite monzogranite is 309 ± 4 Ma, synchronous with the D_2 dextral transpressive event and close to the ages of the eastern Pyrenean plutons, may be slightly older.

Keywords Granite emplacement · Variscan Pyrenees · Zircon U-Pb age · Anisotropy of magnetic susceptibility · Bordères-Louron

G. Gleizes (✉) · G. Crevon
CNRS-UMR 5563 LMTG, Université Paul Sabatier, 14 Avenue Edouard Belin, 31400 Toulouse, France
e-mail: gleizes@lmtg.obs-mip.fr

A. Asrat
Department of Earth Sciences, Addis Ababa University, P.O. Box 1176, Addis Ababa, Ethiopia

P. Barbey
CRPG-CNRS, B.P. 20, 54501 Vandoeuvre-les-Nancy Cedex, France

Introduction

The Hercynian granitic plutonism in the Pyrenees is constituted by about thirty plutons distributed all along the chain, most of them outside the tectono-metamorphic domes (Fig. 1a). They intruded the Paleozoic formations up to the Namurian (Upper Carboniferous). Studies using the anisotropy of magnetic susceptibility (AMS) method were conducted on several plutons as, for example, Cauterets-Panticosa (Gleizes et al. 1998a), Néouvielle (Gleizes et al. 2001) and Quérigut (Auréjac et al. 2004). Reconstruction of their internal structures shows their synkinematic character with a dextral transpressive event (D_2). Zircon U-Pb dating on east Pyrenean plutons shows that they emplaced during the Upper Carboniferous. Available ages are westwards: 307 ± 1 Ma for Saint Arnac (Olivier et al. 2004), 307 ± 3 Ma for Quérigut (Roberts et al. 2000), 305 ± 3 Ma for Mont-Louis-Andorra (Romer and Soler 1995; Maurel et al. 2004) and 312 ± 3 Ma for Bassiès (Paquette et al. 1997). The slightly older age of the Bassiès pluton raises the question of the emplacement ages of plutons in the central and western Pyrenees where U-Pb geochronological data are poorly constrained with two ages in the

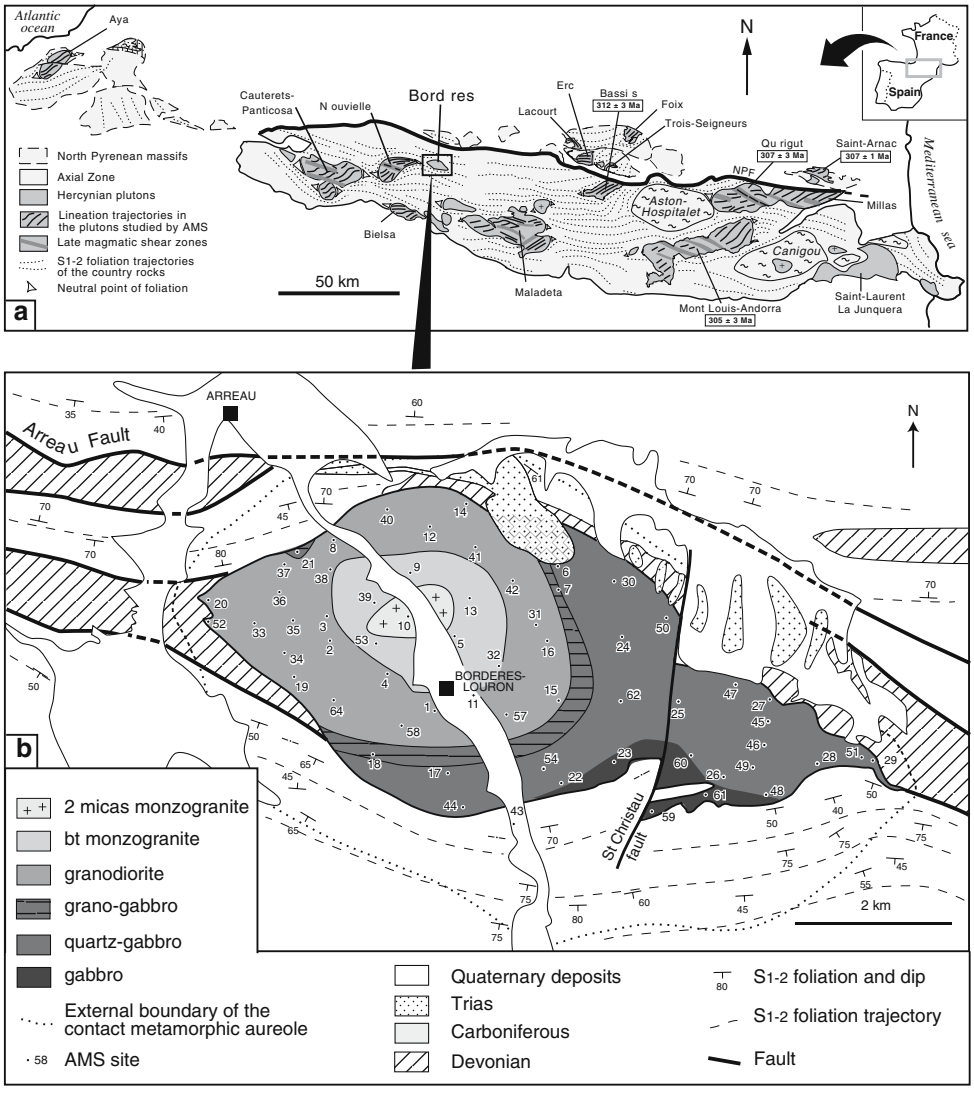

Fig. 1 **a** *Sketch map* of the central and eastern Pyrenees showing the localisation of the granitic plutons and main gneiss domes. **b** Geological map of the Bordères-Louron area modified from Barrère et al. (1984). Lithological limits in the pluton are from Forghani (1964)

eastern part of the Cauterets pluton at 301 ± 7 Ma (Guerrot 1998) and in the Eaux-Chaudes pluton at 301 ± 9 Ma (Guerrot 2001).

Here we present and discuss new structural, AMS and zircon U-Pb data on the Bordères-Louron pluton, located in the Axial Zone of the central Pyrenees (Fig. 1b). This pluton is particularly interesting for two reasons: (1) it displays a complete petrographic zonation from gabbros at the border to two-micas monzogranites in the core, and thus represents an interesting object for studying zonation features, either continuous or discontinuous; (2) it is located in the central part of the Pyrenees and its accurate isotopic dating may allow to check the hypothesis of a diachronism along the belt.

The main results of this study show that this pluton was emplaced in several pulses, quite separated in time, and that the Variscan plutons of the Pyrenees could be possibly older toward the West.

Geological setting

The Bordères-Louron pluton is a 10 × 4 km elliptical body trending N105°E (Fig. 1b). It is concentrically zoned (Forghani 1964), with a core of monzogranites surrounded by granodiorites. Its eastern part consists of (quartz) gabbros representing about one third of the total area, distinguishing it from the other Pyrenean plutons, which comprise more extensive silicic units.

Country rocks consist of Devonian and Carboniferous low grade metasediments affected by cylindrical folds with EW-trending axes (Barrère et al. 1984). A contact metamorphic aureole is observed over a distance of 250–1,800 m all around the pluton, but is much larger in the south (Fig. 1b). Triassic sandstones unconformably overlie the northern contact of the pluton, indicating that it was eroded at the end of the

Hercynian cycle (Lucas 1985). The main structure is a regional S1-2 foliation acquired during the Hercynian tectonics (an early penetrative D1 foliation which suffered a verticalization during the D2 transpression), which led to the large-scale EW structures (Soula et al. 1986; Carreras and Capella 1994). Important EW-trending faults occur in the close vicinity of the pluton (Ternet et al. 1995). Most of them predate pluton emplacement, since the eastern part of the pluton cuts these faults and since the metamorphic aureole is unperturbed by the faults (Fig. 1). Moreover, the gabbros are shifted by a NS-trending fault, the Saint Christau fault, unreported so far. The presence of the Triassic sandstones on both sides of this fault suggests that it could be late-Hercynian in age.

AMS study of the pluton

The AMS method applied to granitoids is detailed in several works which the reader is referred to (e.g. Borradaile and Henry 1997; Bouchez 1997, 2000). It is based on the relations between magnetic and mineral fabrics in magmatic rocks, as shown from image processing (e.g. Launeau et al. 1994). Briefly, two or three oriented cores (25 mm in diameter) were drilled at each site. In the laboratory, two or three specimens (22 mm long cylinders) were cut from each core. Each specimen was measured for its AMS at low field ($\pm$ 4.10^{-4} T; 940 Hz), using a Kappabridge KLY-2 susceptometer following the procedure of Jelinek (1978). Measurements result in the orientation and magnitude of the three main axes $K_1 \geq K_2 \geq K_3$ of the magnetic susceptibility ellipsoid. Their vectorial mean measured on all the specimens of each site defines the mean ellipsoid representative of the magnetic fabric of the site. From this ellipsoid are calculated the average susceptibility value ($K_m = (K_1 + K_2 + K_3)/3$), magnetic lineation ($K_1$) and foliation (plane normal to K_3), percentage of anisotropy (Ppara% $= 100 \times [(K_1 - D)/(K_3 - D) - 1]$) and shape parameter $[T = \ln[K_2^2/(K_1 \times K_3)]/\ln(K_1/K_3)]$. D corresponds to the diamagnetic contribution of quartz and feldspars, which is considered to be constant and estimated at -14×10^{-6} SI (Rochette 1987). Though Ppara% is clearly related to the amount of deformation, the shape parameter T is much more complex since it depends on both the deformation regime and amount of biotite and amphibole in the specimen.

Gleizes et al. (1993) have shown that the Pyrenean granites are paramagnetic and that the magnetic susceptibility is dominantly related to iron-bearing silicates (biotite, amphibole, clinopyroxene). Therefore, the K_m value is proportional to the iron content and can be correlated to the mineralogical composition. The biotite AMS ellipsoid is flattened ($k_1 = k_2 > k_3$) with a short axis k_3 normal to the (001) plane, whereas the AMS ellipsoid of amphibole is elongated ($k_1 >> k_2 > k_3$), with the long axis k_1 sub-parallel to the crystal [c] axis (Rochette 1987). Hence, K_1 corresponds to the zone axis of biotite flakes and to the mean elongation axis of amphibole, whereas K_3, pole of the magnetic foliation, corresponds to the mean flattening plane of biotite.

Mineralogical composition and magnetic susceptibility

Sixty-two sites were sampled in the Bordères-Louron pluton (Fig. 1b). The mean values of parameters at each site are given in Table 1. Thin sections were made for half the sites in order to control the microstructural state and determine the mineralogical composition of rocks. Microstructures are in most cases magmatic, with the exception of some samples collected at the contact with the country rocks or at the interface between granites and gabbros. These samples show subsolidus deformation microstructures (kinked biotite, broken plagioclase with infilling of quartz and feldspar).

Mineralogical data (Fig. 2) corroborate the concentric zoning described by Forghani (1964). The gabbros contain hornblende and both ortho- and clinopyroxenes, which are commonly rimmed with amphibole. Corona textures occur locally with orthopyroxene rimmed with clinopyroxene and hornblende. The granodiorites contain biotite and hornblende only, with the exception of a few pyroxenes at the contact with the gabbros (Fig. 3). The core of the pluton consists of biotite monzogranite, which may locally contain muscovite. Apatite, ilmenite and zircon are ubiquitous, whereas titanite and allanite occur only locally. Retrogression is limited and corresponds to the transformation of ferromagnesian minerals into chlorite and epidote, and of plagioclase cores into damourite.

A histogram of susceptibility values K_m (10^{-6} SI) shows several spikes corresponding to the different rock types (Fig. 3). The values range from 550–700 in the gabbros to 50–150 in the two micas monzogranites, though the evolution of K_m is not continuous. The different rock types are clearly individualized with well-defined average susceptibility values K_m: 595 $\pm$ 6% for gabbros, 462 $\pm$ 7% for quartz gabbros, 274 $\pm$ 3% for granodiorites and 188 $\pm$ 6% for biotite monzogranites in 90% of the sites. The two micas monzogranites have the highest variability (K_m = 119 $\pm$ 11%). The K_m values are independent of their

Table 1 AMS measurements and petrographic types of the Bordères-Louron pluton

Site	Type	Km	Ppara (%)	*T*	Foliation			Linéation	
1	mg2	118	2.3	0.13	80	S	32	259	0
2	mg	199	1.9	0.21	113	S	77	288	24
3	mg2	139	2.0	0.49	51	N	77	231	19
4	mg	183	3.0	0.76	101	S	55	115[a]	13
5	mg	190	3.0	0.33	43	E	8	26	1
6	gd	278	1.6	0.25	113	N	22	14	26
7	g	553	2.1	−0.04	43	E	85	148[a]	72
8	gdp	306	1.5	0.6	114	N	83	107	62
9	mg	175	3.6	0.57	84	S	61	257	14
10	mg	228	4.6	0.59	119	S	18	227	15
11	mg2	93	3.0	0.52	54	S	54	162	58
12	mg	187	2.2	0.61	97	N	75	94[a]	20
13	mg2	101	2.6	0.38	129	N	59	323	23
14	gd	289	1.7	0.27	95	S	56	126	35
15	gd	280	2.9	0.21	61	S	64	231	21
16	mg	164	2.0	0.64	9	E	54	36	33
17	gd	278	4.0	0.81	83	S	47	91	3
18	gd	271	4.3	0.71	106	S	65	278	17
19	gd	270	2.0	−0.42	122	N	88	308	55
20	qg	489	0.8	−0.13	122[a]	S	23	117[a]	3
21	gdp	302	1.8	0.4	92	S	76	216	71
22	g	648	2.9	0.6	48	S	68	119	65
23	g	553	2.0	0.07	127	N	72	90	56
24	g	588	1.6	−0.03	38[a]	E	19	192[a]	17
25	qg	465	2.5	0.22	137	W	58	147	15
26	qg	498	3.0	0.29	62	S	72	73[a]	10
27	g	559	2.1	0.06	126	N	68	312	7
28	qg	446	1.9	0.29	159[a]	E	71	62	30
29	qg	409	1.1	−0.2	26	E	18	150	16
30	qg	491	1.3	0.1	4	E	59	154	43
31	mg	180	1.2	−0.08	122	S	74	160	63
32	mg	186	2.6	0.61	84	S	50	109	28
33	gd	264	1.3	0.21	170	E	42	137	34
34	mg	186	3.0	0.38	146	W	72	317	27
35	mg	207	3.2	0.75	177[a]	W	85	158[a]	2
36	mg	195	2.6	0.53	144	W	71	166	49
37	mg	193	2.1	0.43	13	E	80	184	41
38	mg	185	2.2	0.02	43	W	89	226	69
39	mg2	121	3.2	0.39	161	W	39	278	34
40	gd	288	1.9	0.39	78	S	71	250	26
41	mg	189	1.6	0.11	118	S	74	135	42
42	mg	182	2.3	0.52	63	S	64	237	14
43	g	644	3.8	0.51	101	S	80	265	55
44	gdp	332	3.0	0.06	67	S	83	246	7
45	qg	490	1.4	−0.09	147[a]	W	64	166[a]	35
46	qg	511	3.2	0.5	174	E	71	162	33
47	qg	418	3.4	0.36	135	W	80	313	14
48	qg	474	1.8	0.43	94	N	56	286	10
49	qg	495	2.5	0.72	162	E	83	345	33
50	qg	387	1.7	−0.02	147	W	35	248	34
51	qg	424	0.9	0.01	35[a]	E	27	37[a]	23
52	gdp	311	3.6	0.66	2	W	87	0	24
53	mg2	122	5.0	0.09	133	S	14	190	7
54	gdp	344	3.9	−0.37	28	E	63	201	15
57	gd	272	3.5	0.66	50	S	49	214	19
58	mg	161	2.9	0.71	100	S	50	180	52
59	qg	455	1.6	0.32	77	S	76	258	10
60	g	633	2.0	0.19	79	S	50	118	32
61	qg	476	1.1	0.29	64	N	21	33	9
62	g	581	1.9	0.1	88	N	18	5	17
63	mg2	137	6.6	0.17	121	S	37	205	37
64	gd	254	3.6	0.64	123	N	43	318[a]	25

mg2 Two-micas monzogranite, *mg* bt monzogranite, *gd* granodiorite, *gdp* clinopyroxene granodiorite, *qg* quartz gabbro, *g* gabbro

[a]Ill-defined site

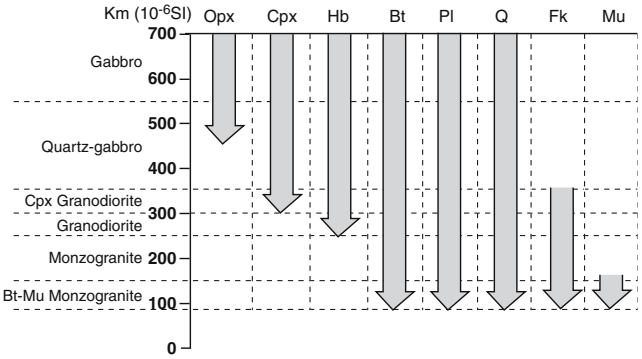

Fig. 2 Correlation between the mineralogical composition and the magnetic susceptibility (K_m) of the different lithologies of the Bordères-Louron pluton. *Opx* Orthopyroxene, *Cpx* clinopyroxene, *Hb* hornblende, *Bt* biotite, *Pl* plagioclase, *Q* quartz, *Fk* alkali feldspar, *Mu* muscovite

location within the same rock unit, suggesting that there is no significant zoning within each unit. Comparison with thin sections shows that orthopyroxene disappears for $K_m < 450 \times 10^{-6}$ SI, clinopyroxene below 300 and hornblende below 250 (Fig. 2). K-feldspar appears for $K_m < 350$ and muscovite for $K_m < 170$. These values are comparable to those reported in other Hercynian plutons of the Pyrenees (e.g. Gleizes et al. 1993).

Comparison of mineralogical and susceptibility data allows the lithological map published by Forghani (1964) to be improved. This highlights the interest of the AMS technique, which is based on numerous sampling sites and on a very good correlation between the susceptibility values and the petrographic types for the paramagnetic granitoids (Gleizes et al. 1993).

The main differences are the existence of the NS-trending St Christau fault, the wider extension of the biotite monzogranite and two micas monzogranite, and the absence of quartz gabbros along the south-eastern border. Two major lithological units are visible: (1) gabbros to the east forming a wedge cut into two parts by the St Christau fault (quartz gabbro to the east and mainly gabbro to the west); and (2) granites to the west, which are nested in concentric ellipses with their long axes coinciding with the pluton axis (N100°E). The peripheral granodiorite has a variable width (10–1,000 m) and is rimmed by pyroxene granodiorite along the gabbros and along the southern border with the country rocks. The distribution of the two micas monzogranite may correspond to local bulges of its roof.

Magnetic foliation and lineation

Magnetic foliation and lineation (Fig. 4) are parallel to those of minerals as the rocks display a dominant paramagnetic behaviour. The magmatic nature of the microstructures indicates that they are likely to represent, respectively, the flattening plane and the stretching direction of magmas in the last stages of crystallization.

Foliation poles are dispersed (Fig. 4a). Silicic and mafic rocks show distinct patterns on the map. In granites, foliation trajectories form a rough elliptical dome with a N95°E-trending long axis, centerd on the monzogranite core where dips are near-horizontal. Toward the periphery, foliation dips outwards with increasing values. It becomes vertical and then inverts

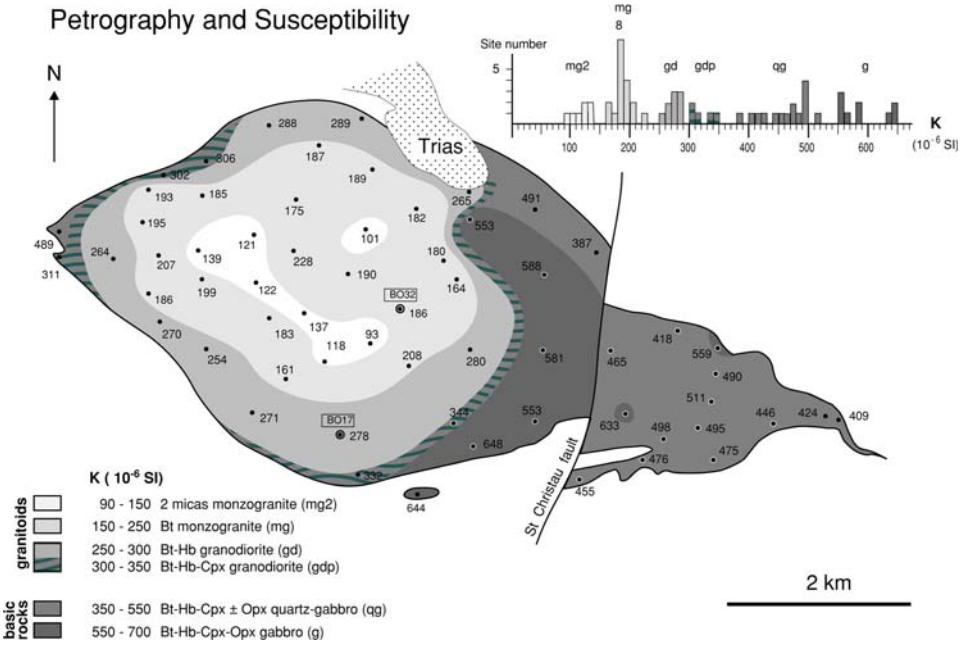

Fig. 3 Map of magnetic susceptibility of the Bordères-Louron pluton. Relationship between susceptibility and lithology is indicated. *Inset* Histograms of susceptibility values. *BO17* and *BO32*: samples for the U-Pb dating

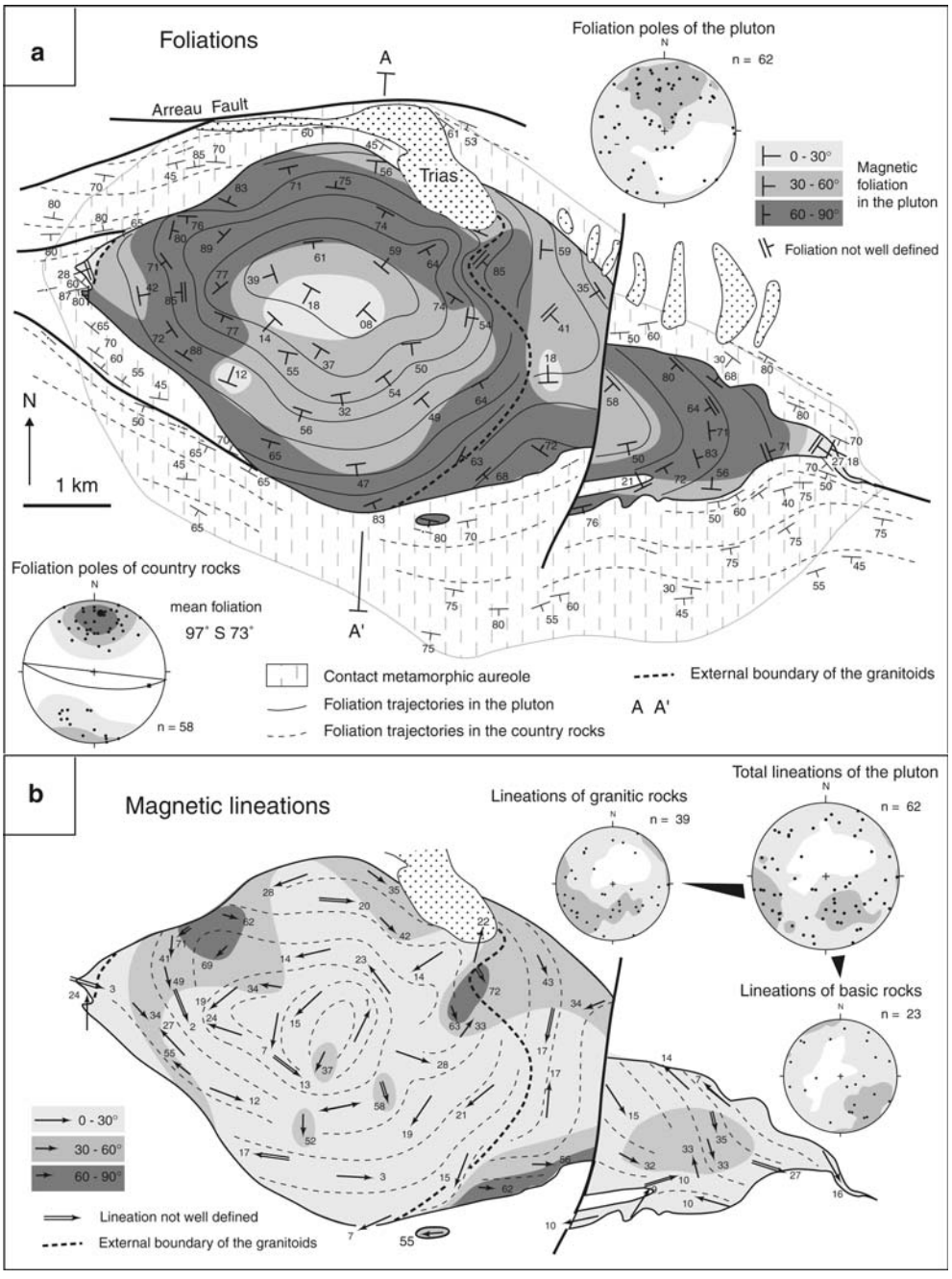

Fig. 4 Maps of magnetic foliations (**a**) and lineations (**b**) of the Bordères-Louron pluton

to become centripetal in the granodiorite along the northern and western borders. In the gabbros, data are much more scattered and some of them are not well defined. However, to the west of the St Christau fault, the structures of granodiorite and gabbros are to some extent in accordance. To the east, the structure characterized by steep dips can fit together with the one of the opposite compartment by southward displacement. In the contact aureole, the fabric is very planar and lacks lineation. On the whole, the foliation wraps around the pluton as shown by foliations trajectories (Fig. 4a), and has a mean orientation of 97° S 73°.

Lineations are also scattered and their trajectories roughly follow those of the foliation ones, with predominantly low dips (< 30°). Moderate plunges (30°–60°) are located within a peripheral band in the north and west. The steep dips (> 60°) occur only in two limited areas in the NW and NE, where the width of the granodiorite ring is restricted to some tens of meters. In the gabbros, the mean lineation plunges slightly to the SE. In the western compartment of the St Christau fault, lineation trajectories are parallel to those of the granites with low dip in the core, moderate in the north and steep in the south at odds with the

granites. In the eastern compartment, trajectories are NW–SE with a distinct distribution of dips, which are generally low with the exception of the core where they are moderate.

It is worth noting that in gabbros, where magnetism is linked to clinopyroxene, lineations of the four specimens of same site are closely grouped. As clinopyroxene crystals are statistically in line with the stretching lineation, this means that despite the obliquity (~ 45°) of its magnetic K_1 with respect to its long geometrical axis (Lagroix et al. 2000), they get in zone around this axis. Hence, the resultant of the K_1 values is coaxial with the mean alignment of the pyroxene crystals. The coherence of the results obtained for the dominantly paramagnetic Bordères gabbros validates the AMS technique for this kind of rocks.

Intensity and shape of the magnetic fabric

The distribution of anisotropy susceptibility values Ppara% (Fig. 5) shows that granites (average Ppara% = 2.8) are more anisotropic than gabbros (average Ppara% = 1.9). In granites, values range from 1.2 to 6.6, being < 2 for 24% of the sites and > 3 for 42%. In mafic rocks, Ppara% values range from 0.8 to 3.4, being < 2 for 54% of the sites and > 3 for only 14%. The higher anisotropy values (> 4%) occur in both the granodiorite to the south of the pluton close to the contact, and the biotite monzogranite in the core close to the two-mica monzogranite. On the whole, the anisotropy intensity decreases toward the contact to < 2% in the peripheral granodiorite (with the exception of the southern granodiorite). In the gabbros to the west of the St Christau fault, anisotropy values are in most cases < 2%, with the exception of the southern contact where it reaches 2.9% (3.8% in a small outcrop to the south of the pluton). To the east of the fault, values are rather high (> 3%) in the core and in the north. Lastly, the lowest values (< 1%) occur in the quartz gabbros of the eastern and western tips of the pluton.

Values of the shape parameter (Fig. 5b) spread over a large interval for both granites ($-0.42 < T < 0.81$) and gabbros ($-0.20 < T < 0.72$), suggesting that it is to some extent independent of the mineralogical composition. The fabric appears to be mainly planar to very planar in granites ($T_{aver} = 0.4$, $T > 0.5$ in 46% of the sites and negative in 5% only), whereas it is mainly planar to linear in gabbros ($T_{aver} = 0.17$, $T > 0.5$ in 16% of the sites and negative in 29%). In detail, some points should be emphasized:

1. In granites, the fabric tends to be less planar toward the gabbros and may even become locally linear at their contact and in the pyroxene granodiorite rim. The very planar fabrics seem to surround the two-micas granites.
2. In gabbros, the fabric differs from one side of the St Christau fault to the other. In the west, fabric is almost exclusively linear, with the exception of the southern border, where it is strongly planar ($T = 0.6$), and of the small isolated outcrop ($T = 0.51$). In the east, fabric is mainly planar, with the exception of the NE and in the tip where it is linear.

Zircon U-Pb data

Zircons were separated from two samples (monzogranite, granodiorite). Crystals were selected from 50 to 150 μm fraction extracted from 10 kg of each sample, using heavy liquids and a Frantz magnetic separator. Zircons were hand-picked using a binocular microscope and were selected by choosing the limpid, euhedral grains with well developed prisms. They contain very low amounts of primary cracks and inclusions (apatite, quartz, mica). Selected zircons were mounted in epoxy resin together with fragments of the 91500 standard zircon (Ontario, Canada), with an age of 1062.4 ± 0.4 Ma (Wiedenbeck et al. 1995). Mounts were then polished and gold coated. In back-scattered electron microscopy, zircons show a thin oscillatory zoning of magmatic origin (Fig. 6) and in some cases rounded cores.

U-Pb isotopic compositions were measured on zircon single grains using the CRPG Cameca IMS-1270 ion microprobe (Nancy). Instrumental conditions and data reduction procedures are detailed in Deloule et al. (2002). Correction for common lead was made by measuring the ^{204}Pb content, and the common lead composition was estimated at the $^{207}Pb/^{206}Pb$ measured age using the model of Stacey and Kramers (1975). Isotopic data along with uncertainties and ages are given in Table 2. Concordia diagrams and discordia lines (Figs. 6, 7) were constructed using the Isoplot3 program (Ludwig 2003). Because $^{207}Pb/^{235}U$ ratios are more sensitive to common lead correction, we consider, following Deloule et al. (2002), the individual $^{206}Pb/^{238}U$ ages as more reliable.

Zircons from the monzogranite consist of five core-free grains (3,242, 3,261, 3,266, 3,269, 3,275) yielding concordant $^{206}Pb/^{238}U$ ages ranging from 308 to 311 Ma, one rounded core (3,288) with a concordant $^{206}Pb/^{238}U$ age of 586 ± 10 Ma, and one slightly discordant grain (3,268). The weighted average of the five concordant grains is 309.4 ± 3.9 Ma (MSWD = 0.11). Zircon data from the granodiorite

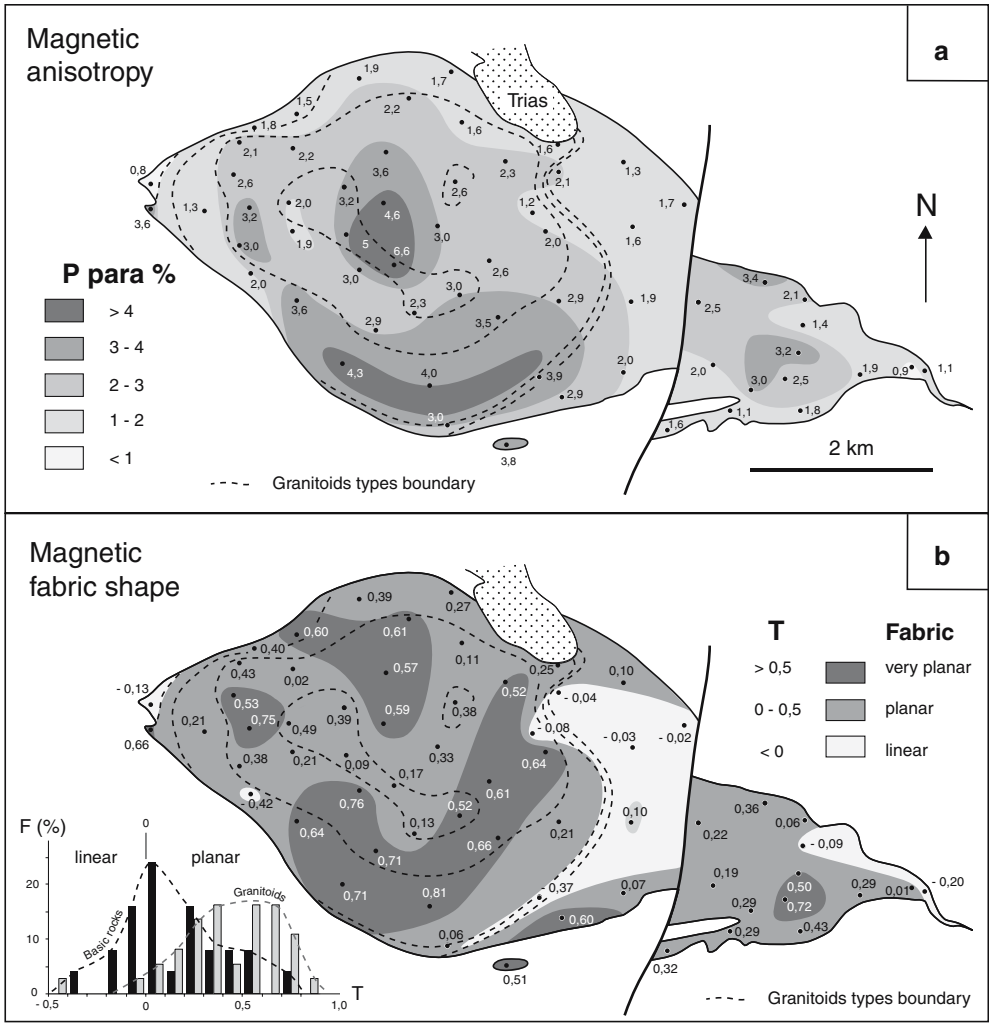

Fig. 5 Maps of magnetic anisotropy Ppara% (**a**) and shape parameter T (**b**) of the Bordères-Louron pluton

(Fig. 7) show significant scatter and do not allow a precise age to be defined. Two concordant grains (1,717, 1,782) and one subconcordant grain (1,703 below the Concordia) yield a weighted average of 321 ± 6 Ma. A subconcordant grain (1,706) with a $^{206}Pb/^{238}U$ age of 271 Ma is in line with four discordant grains (1,702, 1,705, 1,716, 1,729). A concordant grain (1,709) gives an age of 388 ± 2 Ma.

These data led us to consider that the 309.4 ± 3.9 Ma value is likely to be the age of emplacement and crystallisation of the monzogranite pulse. This age is in satisfactory agreement with zircon U-Pb ages on similar granite massifs from the eastern Pyrenees, although slightly older. Inheritance at 586 Ma is in close agreement with previous data indicating a Pan-African/Cadomian inheritance (Laumonier et al. 2004; Cocherie et al. 2005). The emplacement age of the granodiorite is much more uncertain, but could be possibly older than the monzogranite in agreement with field relationships. The other data suggest a complex pattern of inheritance and lead loss, with a possible indication of a Permian event.

Discussion

Pluton construction

Our data suggest that the Bordères-Louron pluton results from the emplacement of two distinct units in two distinct episodes, as envisionned by Debon et al. (1996), rather than from a continuous emplacement sequence as suggested by Forghani (1964).

1. In spite of a limited number of data, there is a clear gap between the lower K_m values in the quartz gabbros (387×10^{-6} SI) and the upper ones in biotite-hornblende granodiorites (289×10^{-6} SI).
2. In the granites, the gap is much narrower (20×10^{-6} SI), but the distribution of K_m values (histogram of Fig. 3) also suggests independent injections. Moreover, we have seen that the variability of K_m in the granodiorite and biotite

monzogranite is low (< 10%), that is on the order of the intrinsic variability in a site.

3. The decametre-wide ring of clinopyroxene granodiorite, in between granites and gabbros, is likely to result from mixing in the contact zone of the two magmas. The K_m values for this rim (302–344 $\times 10^{-6}$ SI) are intermediate between those of the quartz gabbro and the granodiorite, though closer to the granodiorite values. Note that the occurrence of this rim at the contact with the country rocks could suggest the presence of gabbros at shallow depth.
4. Two zones of constriction in the granodiorites, in the NW and NE (Fig. 3), suggest that the granodiorite magma was flattened out against gabbros already largely crystallized. In these two areas, the structures of granodiorites are perturbed, with very steep foliations and lineations (Fig. 4). Constriction could result from inflation related to forceful injection of monzogranitic magmas within the granodioritic one. Therefore, the emplacement succession could be gabbroic, granodioritic and monzogranitic magmas. The regularity of the geometric relationships between the different magma batches suggests that mafic magmas were mostly non-solidified when the last injection of granite occurred, and that the successive episodes of injection rapidly followed each other.

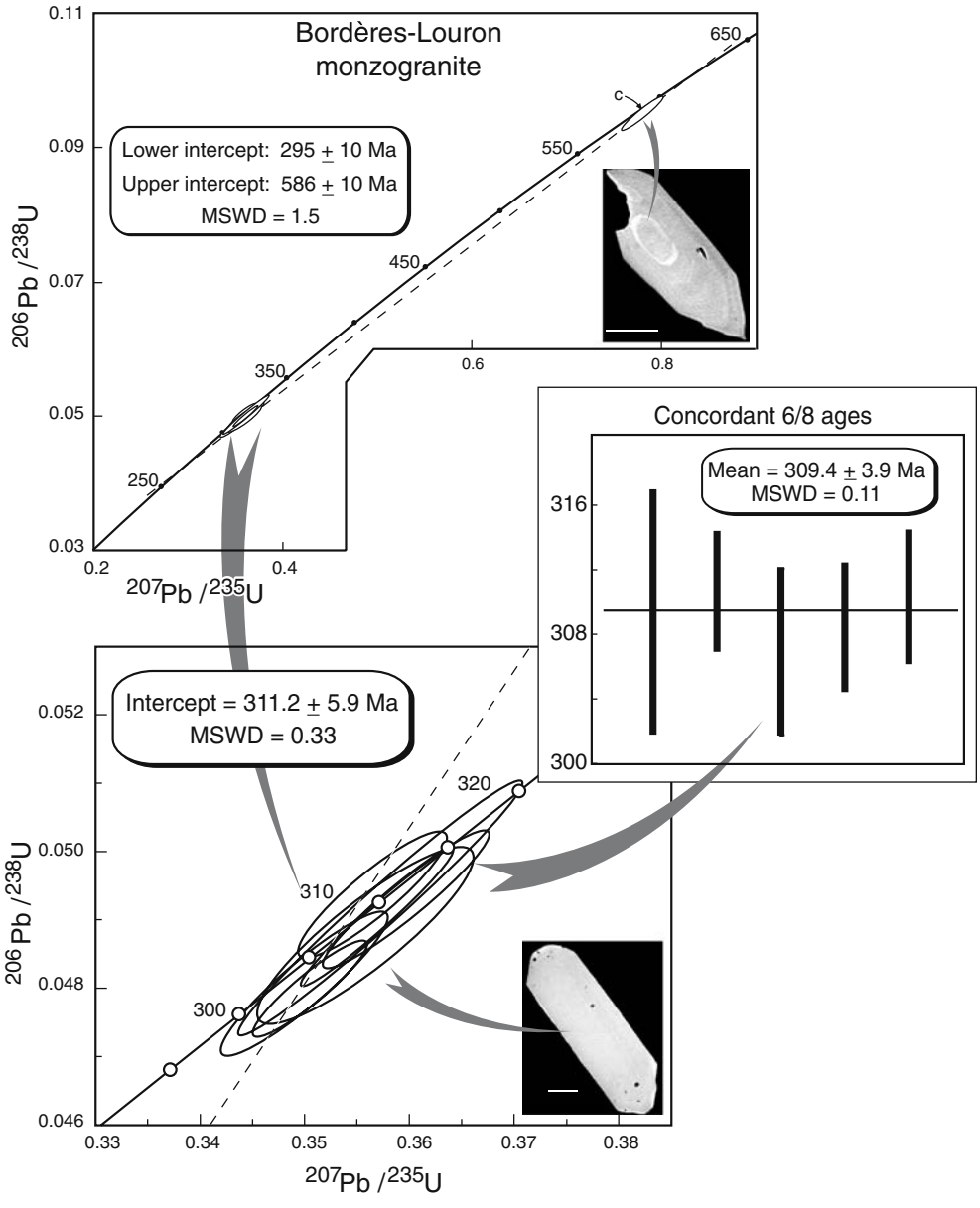

Fig. 6 Concordia diagrams for zircons and mean $^{206}Pb/^{238}U$ of the concordant values for the Bordères-Louron monzogranite (*c* denotes core of zircon grains)

Table 2 U-Pb isotopic data for the zircons analyzed

Analytical spot	$^{206}Pb/^{204}Pb$ measured	Concentration (ppm)			Corrected ratios				
		Pb	U	Th	$^{206}Pb/^{238}U$	$\pm \sigma$	$^{207}Pb/^{235}U$	$\pm \sigma$	$^{207}Pb/^{206}Pb$
3242-16	3,474	8	182	90	0.0494	0.0006	0.3564	0.0048	0.0524
3261-15	6,466	17	409	225	0.0492	0.0012	0.3571	0.0091	0.0527
3269-14	15,750	39	925	807	0.0490	0.0006	0.3568	0.0047	0.0528
3266-11	3,151	8	180	105	0.0488	0.0008	0.3558	0.0068	0.0529
3268-12	10,581	25	596	397	0.0480	0.0005	0.3505	0.0036	0.0530
3275-10	3,447	9	202	103	0.0493	0.0007	0.3596	0.0052	0.0529
3288-6[a]	9,136	49	596	157	0.0951	0.0016	0.7866	0.0142	0.0600
1706-20	3,579	21	570	220	0.0430	0.0006	0.3098	0.0045	0.0523
1736-18	3,401	9	217	98	0.0481	0.0007	0.3498	0.0053	0.0528
1729-14	2,541	10	250	29	0.0449	0.0003	0.3342	0.0037	0.0540
1717-10	4,997	18	420	36	0.0509	0.0013	0.3763	0.0102	0.0536
1716-9	2,017	7	156	38	0.0504	0.0003	0.3942	0.0032	0.0567
1709-8[a]	2,178	13	251	22	0.0620	0.0004	0.4657	0.0055	0.0545
1705-6	2,789	13	327	38	0.0470	0.0006	0.3547	0.0056	0.0548
1703-5	1,317	7	159	20	0.0519	0.0008	0.3849	0.0086	0.0538
1702-4	1,710	7	181	29	0.0464	0.0005	0.3508	0.0059	0.0548
1782-2	2,911	8	175	100	0.0506	0.0007	0.3700	0.0056	0.0531

The reported errors include the calibration uncertainties

[a]Zircon core

Significance of the intensity and shape of the magnetic fabric

Various studies have shown that the anisotropy value Ppara% in paramagnetic plutonic rocks, which reflects the degree of organization of minerals with shape anisotropy in rocks, can be correlated to the fabric intensity (e.g. Gleizes et al. 2001; Auréjac et al. 2004). If a strong anisotropy reflects a strong deformation, we have a means to quantify the amount of deformation recorded at the magmatic stage or under subsolidus conditions. In the case of the Bordères-Louron pluton, the magmatic nature of microstructures suggests that the different magmas did not suffer further significant deformation once crystallized. Consequently, scalar AMS parameters can be interpreted in terms of deformation recorded by magmas during their emplacement until they fully crystallized.

The strong increase of Ppara% in the southern granodiorite (Fig. 5b) with respect to the rest of the pluton where this parameter is low, indicates a higher amount of deformation in the southern border of the pluton. In the same way, the high anisotropy in the core of the pluton can be related to a higher deformation at the top of the pluton close to the two micas monzogranites. There is also an increase of the anisotropy in the gabbros near the southern border to the west of the St Christau fault. This suggests that they underwent similar deformation as granites. In the eastern compartment (on the whole more anisotropic), the anisotropy maximum in the core seems to be equivalent to the strong anisotropy of the monzogranite core. However, there is a reverse distribution of the anisotropy values which are high in the north and low in the south.

We have seen that the granites show a fabric generally planar, whereas gabbros have a linear fabric (Fig. 5b). This is linked at least partly to their distinct mineralogy. Indeed, the susceptibility of granites is mainly related to biotite (intrinsic planar magnetic anisotropy), whereas that of gabbros is related to pyroxene and amphibole (intrinsic linear anisotropy). Therefore, in similar conditions of deformation, the fabric of granites is likely to be much more planar than that of gabbros. In the Pyrenees, the shape parameter T is in general close to 0 in gabbros and $0 < T < 0.5$ in granites. We therefore consider that fabrics are indicative of a specific regime of deformation (i.e., flattening or constriction) only when they are very planar or linear in granites, and planar to very planar in gabbros. In the Bordères-Louron pluton, the variability of the T parameter is as high in the granites as in the gabbros and ranges from strongly linear to very planar.

The fabric is strongly planar in most biotite monzogranites (Fig. 5b), which were thus essentially flattened. This flattening may be related to the ballooning effect induced by emplacement of the two micas monzogranites. The very planar fabric of the southern

		Ages (Ma)						
±σ	Correl. error	$^{207}Pb/^{206}Pb$	± σ	$^{206}Pb/^{238}U$	± σ	$^{207}Pb/^{235}U$	± σ	Conc.
0.0058	0.9003	301.1	12.5	310.7	3.7	309.6	3.6	103.2
0.0050	0.9800	315.1	10.9	309.4	7.5	310.0	6.7	98.2
0.0024	0.9834	320.0	5.2	308.5	3.9	309.8	3.5	96.4
0.0088	0.8898	324.8	18.5	307.0	5.1	309.1	5.1	94.5
0.0038	0.9282	327.4	8.6	302.2	2.8	305.1	2.7	92.3
0.0051	0.9363	324.0	10.9	310.3	4.1	311.9	3.9	95.8
0.0055	0.9528	603.6	11.6	585.5	9.6	589.3	8.0	97.0
0.0064	0.8957	298.8	14.2	271.1	3.4	274.0	3.5	90.7
0.0058	0.9261	319.2	11.9	302.7	4.2	304.6	4.0	94.5
0.0089	0.5930	371.0	18.8	283.0	1.8	292.8	2.8	76.2
0.0066	0.9699	353.7	14.5	320.2	8.2	324.3	7.5	90.5
0.0049	0.7909	480.7	10.1	317.0	2.0	337.4	2.3	66.0
0.0103	0.4862	389.9	20.7	388.0	2.2	388.2	3.8	99.5
0.0099	0.7824	403.5	20.2	295.8	3.6	308.3	4.2	73.3
0.0163	0.6787	363.6	34.2	325.9	4.8	330.6	6.3	89.6
0.0123	0.6799	404.5	25.2	292.5	3.2	305.3	4.4	76.2
0.0064	0.9072	332.0	13.2	317.9	4.3	319.6	4.2	95.8

granodiorites also suggests local deformation with a high flattening component. Besides, the less planar fabric or linear nature of the fabric of the pyroxene granodiorite may be ascribed partly to the higher amount of amphibole. In the gabbros to the west of the St Christau fault, the strongly planar fabric close to the southern border suggests strong flattening. The eastern gabbros are more planar. A vertical shift could explain the contrast between the two compartments visible on all maps.

Alpine rotation of the pluton and its surroundings

Several arguments suggest Alpine tilting of both the pluton and its surroundings toward the north.

1. The Triassic sandstones show an average dip of 35° toward the NNE (Lucas 1985). On Fig. 8, we present a NS cross-section (located on Fig. 4a) through the pluton and its country-rocks in its present position (Fig. 8a) and an untilted cross-section representing the supposed position of the pluton before an Alpine rotation of about 30° to the North around an E-W-trending horizontal axis (Fig. 8b). The discordance of the Triassic sandstones and conglomerates on the granite and surrounding rocks is then subhorizontal on this restored cross-section. This indicates that the E-W-trending symmetry plane of the pluton was probably about 60° northward dipping during the Variscan time. Hence, the present southern border of the pluton was probably located at a deeper level than the northern border.
2. The contact aureole is on the whole twice as wide in the south as in the north (Fig. 1). This can be easily accounted for by distinct cooling rates if the southern part of the pluton was initially at deeper level than the northern part.
3. A further indirect argument appears from the comparison between the Bordères-Louron pluton and other Pyrenean plutons where their southern borders consist mostly of less evolved, strongly anisotropic and planar rock types (e.g. Auréjac et al. 2004). This has been interpreted as the result of an important deformation of magmas at the pluton floor, in relation to a transpressive regime which make them overthrusting to the south. This interpretation is based on the fact that dips are commonly to the north and that the host-rocks present P-T conditions higher in the south than in the north. In the Bordères-Louron pluton, we observe on the southern border, rocks with high anisotropy and flattening. However, the mean dip of the border is moderate to high to the south. This ''anomaly'' can be explained if we assume that the foliation was initially dipping northwards but subsequently tilted during the Alpine events. The small size of the pluton and its shallow erosion level close to the roof do not allow pressure differences to be seen between the south and north.

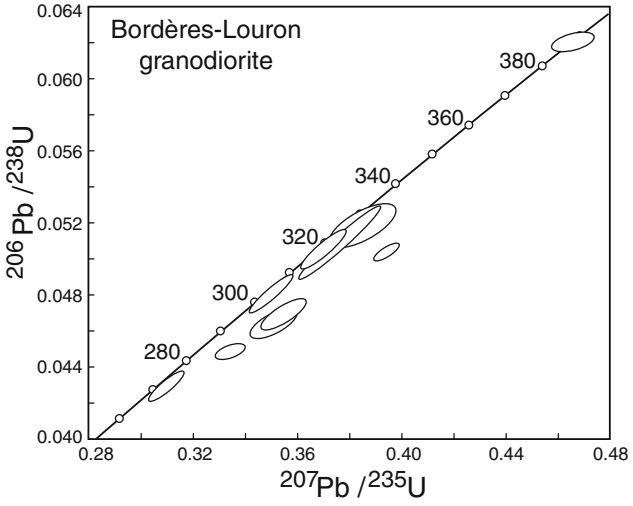

Fig. 7 Concordia diagrams for zircons from the Bordères-Louron granodiorite (*c* denotes core of zircon grains)

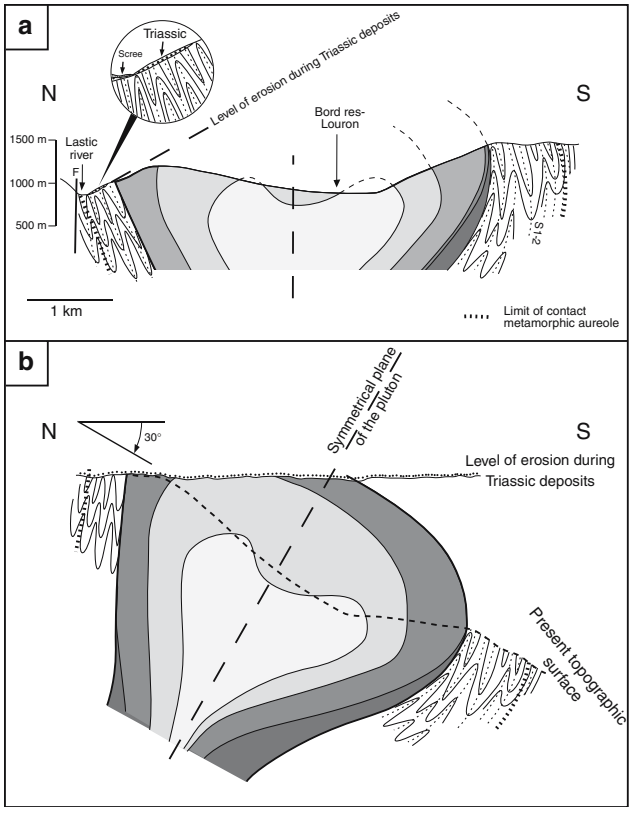

Fig. 8 Cross-section through the Bordères pluton: **a** in its present position, **b** in the position during the Triassic sandstone deposit, after restoration by rotation of about 30° to the South around an E-W trending horizontal axis, corresponding to a supposed Alpine rotation

Mode of emplacement

The overall geometry of the pluton (Figs. 3, 4a), wedge-shaped for the gabbros and dome-shaped for the granites, suggests two distinct modes of emplacement. Low viscosity mafic magmas are likely to use the zones of weakness of the country rocks. Their general EW-trending attitude could suggest that magma injection occurred as a vertical dyke possibly guided by the presence of an early fault zone between the Devonian and Carboniferous sediments, now sealed by the pluton and visible in the western and eastern tips of the pluton (Fig. 1). The tips consisting of quartz gabbros are reminiscent of the tips of a fissure which would have propagated toward the east and west due to magma pressure effect.

The pattern of the granites in concentric ellipses with a foliation roughly parallel to the composite S1-2 foliation in the surrounding country-rocks is synchronous with magma emplacement. The higher viscosity of granitic magmas accounts for the distinct geometry and could be related to successive injections through a conduit located beneath the pluton center.

The 309 ± 4 Ma age of the monzogranite is consistent with an emplacement during the dextral D_2 transpressive event (Gleizes et al. 1998b). Although the lineations are very scattered in the granites, they have a general NE-SW trend (Fig. 4b) which could be the manifestation of the dextral shear component of D_2. Similar patterns were shown in the Cauterets-Panticosa granite complex (Gleizes et al. 1998a) and in the Quérigut pluton (Auréjac et al. 2004).

All the data allow a model of emplacement to be proposed (Fig. 9). Here, we assume that the foliation is in its primary position, i.e. with a steep dip to the north, that the pluton floor is in the south and the roof in the north, and that the magmatic injections took place southwards.

1. Mafic mantle magmas are transferred into the upper crust in response to the D_2 transpressive tectonics and emplaced as gabbro by means of an early EW-trending discontinuity parallel to the regional foliation (Fig. 9a). A second stage of injection leads to emplacement of the quartz gabbro. The dyke extends in an EW direction and its shape is controlled by the foliation of the host rocks (Fig. 9b).
2. A new batch of magma of granodioritic composition, generated in the lower crust possibly according to the model of Roberts et al. (2000), is injected in the western part of the quartz gabbro unit. This unit, which was not yet solidified, is pushed aside by the granodiorite mass (Fig. 9c). Two further injections, which probably went up through the same conduit, enlarge the plutonic body and push aside the surroundings (Fig. 9d). The biotite monzogranites squashed the granodioritic

unit with local constriction, and was subsequently squashed by the two micas monzogranites.
3. The pluton frozen in the present day configuration at the end of the transpressive event is subsequently cut by the late-Hercynian St Christau fault (Fig. 9e). The whole area is finally tilted to the north by about 30° during the Alpine events.

Conclusion

The structural and geochronological study of the Bordères-Louron pluton leads to the following main conclusions.

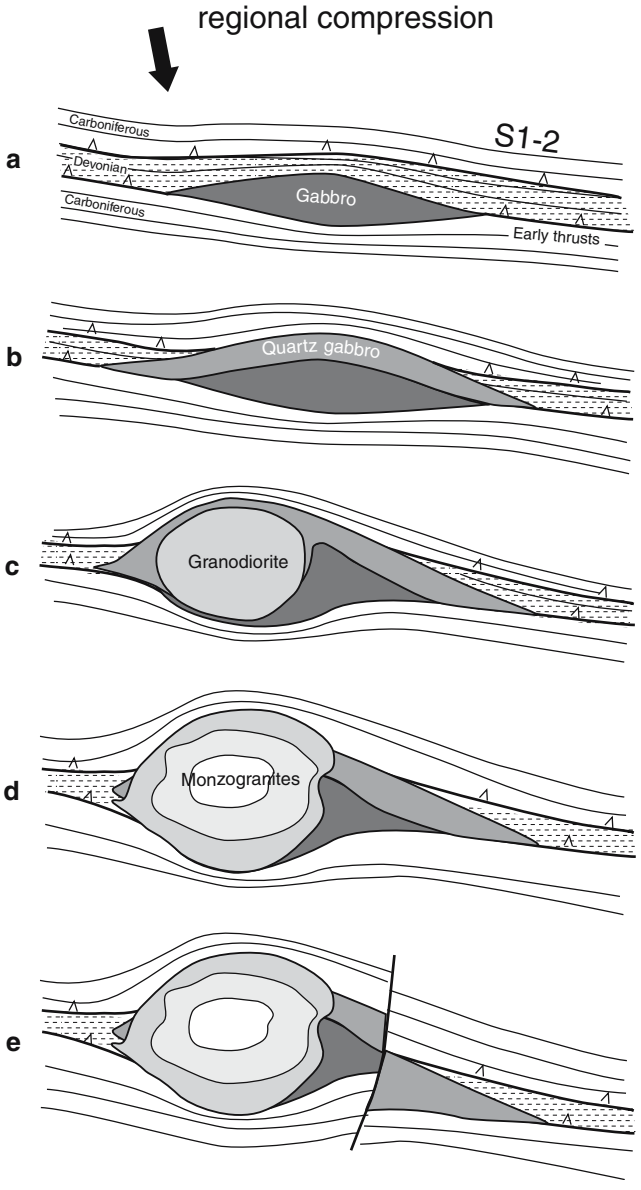

Fig. 9 Cartoon summarizing the successive stages of construction of the Bordères-Louron pluton

1. The study validates the use of the AMS method in the case of gabbros dominated by clinopyroxene. It further shows the interest of scalar parameters (anisotropy intensity, shape parameter) for paramagnetic rocks, which are useful arguments suggesting Alpine tilting of the pluton.
2. In spite of its small size, the Bordères-Louron pluton shows all the lithologies commonly encountered in the Hercynian plutons of the Pyrenees. Its originality lies both in the high proportion of gabbros (emphasizing the role of the mantle in this plutonic event) and in the magmatic nature of the microstructures, which reflect deformation in the late stages of crystallization.
3. The main structural characteristics support emplacement during the D_2 dextral transpressive tectonic event, as formerly reported in the other Pyrenean plutons. The pluton growth results from the discontinuous injection of magmas, first mafic and then granitic, along a crustal discontinuity.
4. Lastly, the zircon U-Pb age of 309 ± 4 Ma can be considered as the age of emplacement. It shows that the plutonism and transpressive tectonics correspond in both the eastern and central Pyrenees to a unique event, which occurred in a limited time span, may be slightly older in the western part than in the eastern part of the range.

Acknowledgments We thank D. Beziat for constructive discussions, R. Peyron and F. de Parseval for thin sections preparation, and C. Cavaré-Hester for her assistance in preparing drawings. This is a contribution of UMR CNRS/UPS 5563 ≪Laboratoire des Mécanismes et Transferts en Géologie≫, Equipe géodynamique.

References

Auréjac JB, Gleizes G, Diot H, Bouchez JL (2004) Le complexe granitique de Quérigut (Pyrénées, France) revisité par la technique de l'ASM: un pluton syntectonique de la transpression dextre hercynienne. Bull Soc Géol Fr 175:65–82

Barrère P et al (1984) Carte géologique de la France (1/50 000), feuille Arreau. BRGM, Orléans

Borradaile GJ, Henry B (1997) Tectonic applications of magnetic susceptibility and its anisotropy. Earth Sci Rev 42:49–93

Bouchez JL (1997) Granite is never isotropic: an introduction to AMS studies of granitic rocks. In: Bouchez JL, Hutton DHW, Stephens WE (eds) Granite: from segregation of melt to emplacement fabrics. Kluwer, Dordrecht, pp 95–112

Bouchez JL (2000) Anisotropie de susceptibilité magnétique et fabrique des granites. C R Acad Sci Paris 330:1–14

Carreras J, Capella I (1994) Tectonic levels in the Palaezoic basement of the Pyrenees: a review and a new interpretation. J Struct Geol 16:1509–1524

Cocherie A, Baudin T, Autran A, Guerrot C, Fanning MC, Laumonier B (2005) U-Pb zircon (ID-TIMS and SHRIMP) evidence for the early Ordovician intrusion of metagranites

in the late Proterozoic Canaveilles Group of the Pyrenees and the Montagne Noire (France): new U-Pb zircon datings. Bull Soc France 176:269–282

Debon F, Enrique P, Autran A (1996) Magmatisme hercynien. In: Barnolas A, Chiron C (eds) Synthèse géologique et géophysique des Pyrénées. Introduction. Géophysique. Cycle hercynien: Edition du Bureau des recherches Géolgiques et Minières et de l'Instituto Tecnologico Geominero de Espana, 729 p

Deloule E, Alexandrov P, Cheilletz A, Laumonier B, Barbey P (2002) In-situ U-Pb zircon ages for Early Ordovician magmatism in the eastern Pyrenees, France: the Canigou orthogneisses. Int J Earth Sci (Geol Rundsch) 91:398–405

Forghani AH (1964) Le massif granitique de Bordères (Hautes-Pyrénées) et son auréole métamorphique. Thèse 3° cycle, Paris

Gleizes G, Nédélec A, Bouchez JL, Autran A, Rochette P (1993) Magnetic susceptibility of the Mont-Louis-Andorra ilmenite-type granite (Pyrenees): a new tool for the petrographic characterisation and the regional maping of zoned granite plutons. J Geophys Res 98:4317–4331

Gleizes G, Leblanc D, Santana V, Olivier P, Bouchez JL (1998a) Sigmoidal structures featuring dextral shear during emplacement of the Hercynian granite complex of Cauterets-Panticosa (Pyrenees). J Struct Geol 20:1229–1245

Gleizes G, Leblanc D, Bouchez JL (1998b) The main phase of the Hercynian orogeny in the Pyrenees is a dextral transpression. In: Holdsworth RE, Strachan RA, Dewey JE (eds) Continental transpressional and transtensional tectonics, vol 135. Geol Soc London, special publications, pp 267–273

Gleizes G, Leblanc D, Olivier P, Bouchez JL (2001) Strain partitioning in a pluton during emplacement in transpressional regime: the example of the Néouvielle granite (Pyrenees). Int J Earth Sci 90:325–340

Guerrot C (1998) Résultats de datation U-Pb par dissolution sur zircons pour le granite de Cauterets, Pyrénées. Rapport inédit, SMN/PEA/ISO 146/98 CG/NB, BRGM. In: Majesté-Menjoulas C, Debon F, Barrère P (eds) Notice explicative, Carte géol. France (1/50 000), feuille Gavarnie (1082). BRGM, Orléans, p 4

Guerrot C (2001) Datation du pluton des Eaux-Chaudes. In: Ternet Y, Majesté-Menjoulas C, Canérot J, Baudin T, Cocherie A, Guerrot C, Rossi P (2004) Notice explicative, Carte géol. France (1/50,000), feuille Laruns-Somport (1069). BRGM, Orléans

Jelinek V (1978) Statistical processing of anisotropy of magnetic susceptibility measured on groups of specimens. Studia Geophys Geod 22:50–62

Lagroix F, Borradaile GJ (2000) Magnetic fabric interpretation complicated by inclusions in mafic silicates. Tectonophysics 325:207–225

Laumonier B, Guitard G, Autran A, Barbey P, Cheilletz A, Baudin T, Cocherie A, Guerrot C (2004) Conséquences de l'absence de socle cadomien sur l'âge et la signification des séries pré-varisques (anté-Ordovicien supérieur) du sud de la France (Pyrénées, Montagne Noire). Bull Soc Géol France 175:643–655

Launeau P, Cruden A, Bouchez JL (1994) Mineral recognition in digital images of rocks: a new approach using multichannel classification. Can Mineral 32:919–933

Lucas Cl (1985) Le grès rouge des Pyrénées. Thèse de doctorat, Toulouse 3

Ludwig KR (2003) User's manual for a geochronological toolkit for microsoft excel. Berkeley Geochronology Center Special Publication, No 4

Maurel O, Respaut JP, Monié P, Arnaud N, Brunel M (2004) U-Pb emplacement and 40Ar/39Ar cooling ages of the Mont-Louis granite massif (Eastern Pyrenees, France). C R Geosci 336:1091–1098

Olivier Ph, Gleizes G, Paquette JL (2004) Gneiss domes and granite emplacement in an obliquely convergent regime: new interpretation of the Variscan Agly Massif (Eastern Pyrenees, France). In: Whitney DL, Teyssier C, Siddoway CS (eds) Gneiss domes in orogeny, vol 380. Geol Soc Am, pp 229–242

Paquette JL, Gleizes G, Leblanc D, Bouchez JL (1997) Le granite de Bassiès (Pyrénées): un pluton syntectonique d'âge westphalien. Géochronologie U-Pb sur zircons. C R Acad Sci Paris 324:387–392

Roberts MP, Pin C, Clemens JD, Paquette JL (2000) Petrogenesis of mafic to felsic plutonic rock associations: the calc-alkaline Quérigut complex, French Pyrenees. J Petrol 41:809–844

Rochette P (1987) Magnetic susceptibility of the rocks matrix related to magnetic fabric studies. J Struct Geol 9:1015–1020

Romer RL, Soler A (1995) U-Pb age and lead isotopic characterization of Au-bearing skarn related to the Andorra granite (Central Pyrenees, Spain). Mineral Deposita 30:374–383

Soula JC, Debat P, Déramond J, Guchereau JY, Pouget P, Roux L (1986) A dynamic model of the structural evolution of the Hercynian Pyrenees. Tectonophysics 129:29–51

Ternet Y, Barrère P, Debroas EJ (1995) Carte géol. France (1/50 000), feuille Campan (1071). BRGM, Orléans

Vitrac-Michard A, Allègre CJ (1975) ^{238}U-^{206}Pb, ^{235}U-^{207}Pb, systematics on Pyrenean basement. Contrib Mineral Petrol 51:205–212